Quantifying emissions from satellite data

Dominik Brunner

Empa, Swiss Federal Laboratories for Materials Science and Technology

With special thanks to Gerrit Kuhlmann and Ronald van der A

Needs of inventory builders and policy makers

- Detection of unknown sources
- Quantification of emission hot spots
- Estimates of relative share of individual emission sectors
- Estimates of total emissions in political unit (country, county, city)
- Changes during last few years (e.g. between reporting periods)
- Long-term emission trends

C40 CITIES

Covenant of Mayors
Committed to local sustainable energy

United Nations Environment Programme
UNEP
WORLD METEOROLOGICAL ORGANIZATION
IG3IS
GLOBAL ATMOSPHERE WATCH

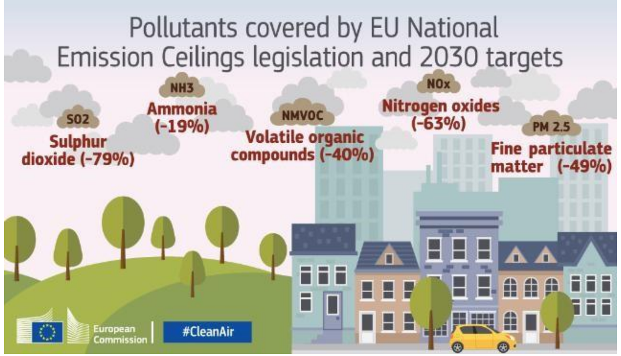

Satellite versus in-situ observations for emission estimation

Satellites

+ Global spatial coverage
+ Representative of large air volume
+ Spatial mapping / imaging
+ Rather uniform quality globally
+ Data access

- Limited temporal coverage, also limited by clouds, daytime (UV/VIS)
- Low spatial resolution
- Small number of species
- Varying vertical sensitivity
- Comparatively low accuracy

Ground-based in situ

+ High temporal resolution
+ All weather measurements
+ High accuracy (potentially)
+ Measurements in PBL near surface
+ Large number of species

- Poor spatial representativeness and coverage
- Diversity of networks & instruments
- Varying data quality

Emission estimation approaches

Mass balance

- Quantify flux divergence

$$Q_c = \left\langle \frac{\partial m}{\partial t} \right\rangle + \int\int\int \nabla \cdot c u \mathrm{d}V = \left\langle \frac{\partial m}{\partial t} \right\rangle + \int_0^{z_{\max}} \oint c' u_{\mathrm{h}} \cdot \hat{n} \mathrm{d}l \mathrm{d}z$$

Volume integral

Surface integral

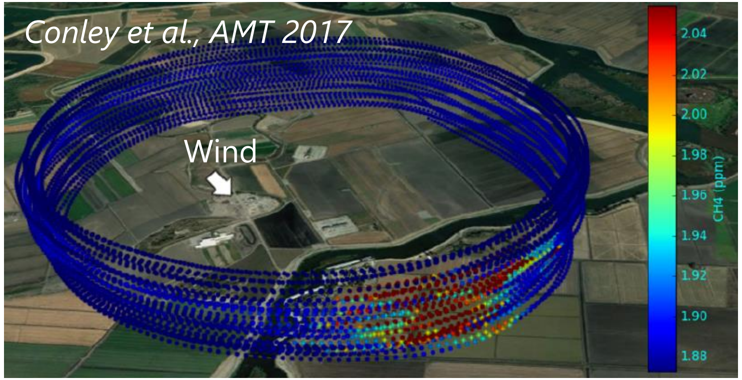

Inverse modelling

- Atmospheric transport model
- Bayesian inversion, Kalman filter, etc.

$$J = \frac{1}{2}(\mathbf{Hx} - \mathbf{y})^T \mathbf{R}^{-1}(\mathbf{Hx} - \mathbf{y}) + \frac{1}{2}(\mathbf{x} - \mathbf{x_a})\mathbf{B}^{-1}(\mathbf{x} - \mathbf{x_a})$$

Observation and model uncertainty

Prior emission uncertainty

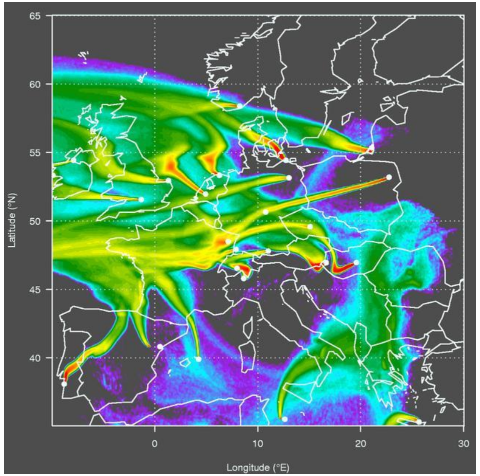

Source-receptor relationship **H** from FLEXPART Lagrangian backward transport simulations

Early example of NO_x emission estimation

Martin et al., JGR 2003

- Estimation of global NO_x emissions using GOME NO_2 observations and global GEOS-CHEM model
- Assumes that NO_x emitted in column is chemically depleted within the same column due to short lifetime

$$E_t = \alpha \Omega_r \qquad \alpha = (\Omega_{NO_x} / \Omega_{NO_2}) / \tau_{NO_x}$$

NO_x emission

Measured NO_2 column

NO_x lifetime

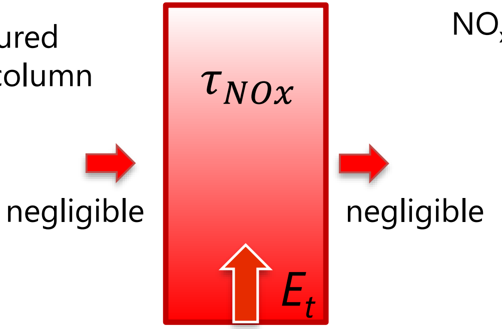

A priori (EDGAR)

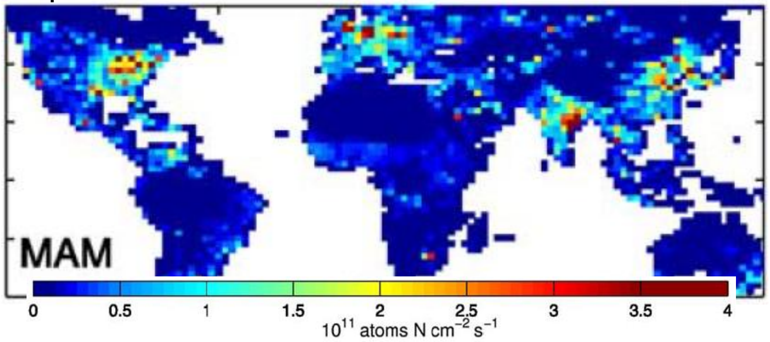

A posteriori - a priori

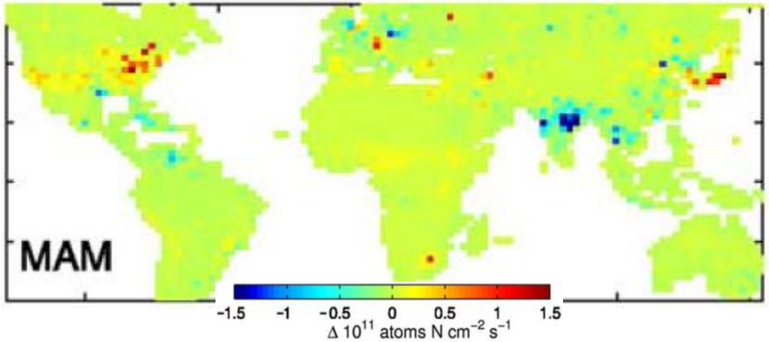

Recent example of NO_x emission estimation

EUMETSAT Empa Materials Science and Technology

DECSO algorithm (Mijling et al., JGR 2012)

- Mixed Eulerian – Lagrangian approach
- Accounts for transport and chemical decay
- Kalman filter

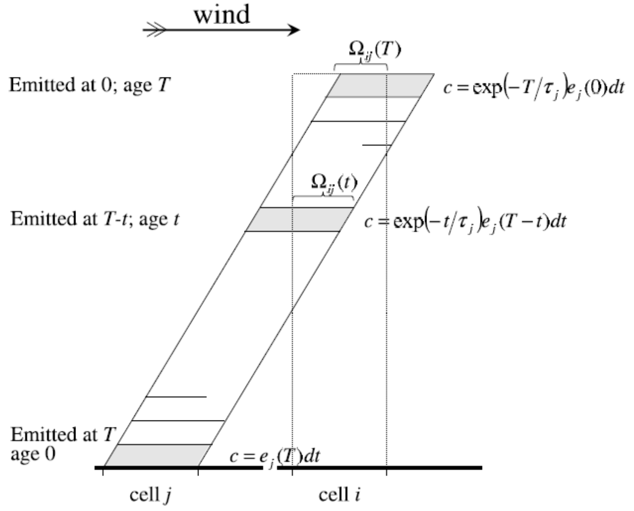

$$\mathbf{c}(T) = \mathbf{G}\mathbf{c}(0) + \mathbf{H}\mathbf{e}$$

Columns at time T (= 24 h) | Columns at time 0 | Emissions btw. 0 and T

Decay of NO_x originating in cell j during transport to cell i over time T

$$G_{ij}(k_j) = \frac{a_j}{a_i} e^{-k_j T} \Omega_{ij}(T)$$

Decay of emissions in cell j during transport to cell i

$$H_{ij}(k_j) \approx \frac{a_j}{a_i} \sum_{n=1}^{n_T} e^{-k_j t_n} \Omega_{ij}(t_n) f_j(T - t_n) \Delta t$$

Sentinel–5P NO2, April 2018 – March 2019

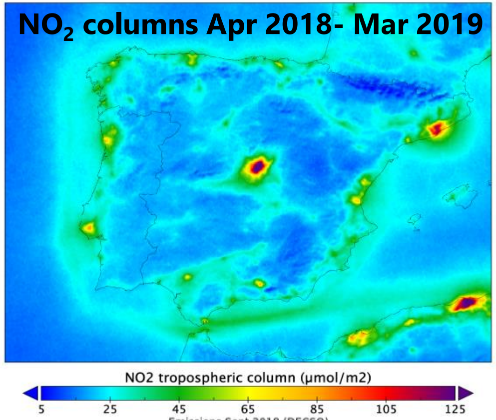

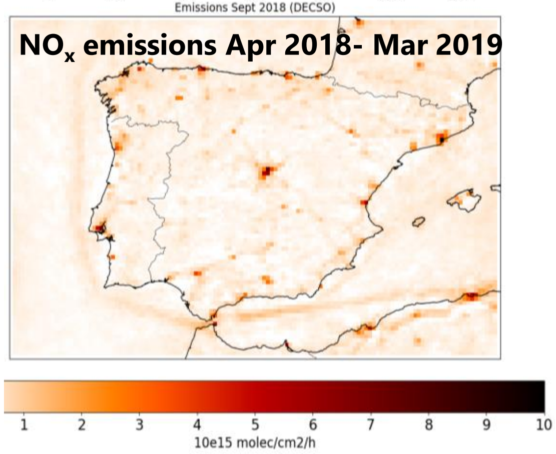

Credit: Ronald van der A

Recent example of NO_x emission estimation

van der A et al., npj Clim. Atm. Sci. 2019

- Quantification of NO_x emissions along a West Siberian natural gas pipeline
- TROPOMI NO_2 observations, new retrievals over snow-covered surfaces
- DECSO algorithm for emission quantification

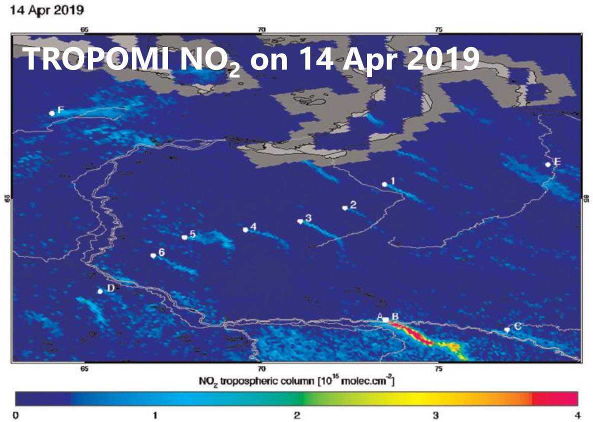

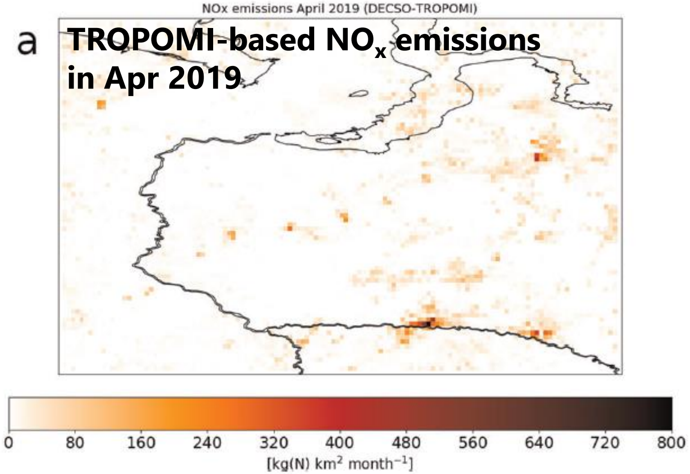

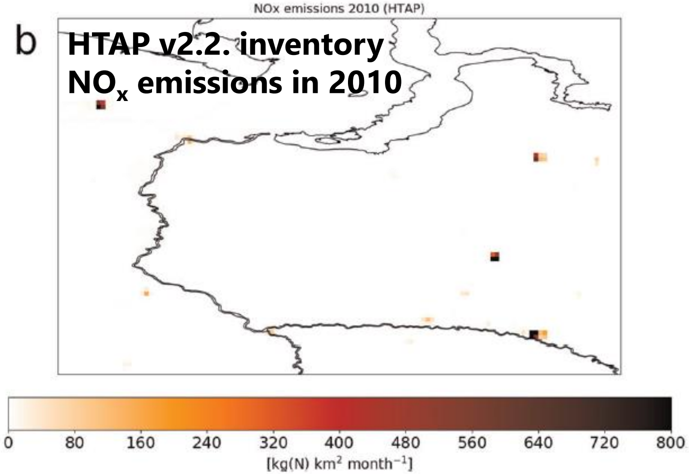

SO_2 point source emissions

Fioletov et al. GRL 2015

- Estimation of point source SO_2 emissions from OMI observations
- Simultaneous fitting of emission, lifetime, and dispersion
- Rotation of plumes to have common wind direction
- Mathematical description of a dispersing and decaying plume

$$\mathrm{OMI}_{SO_2}(x,y,s) = a \cdot f(x,y) \cdot g(y,s)$$

$$f(x,y) = \frac{1}{\sigma_1\sqrt{2\pi}} \exp\left(-\frac{x^2}{2\sigma_1^2}\right);$$

Gaussian dispersion

$$g(y,s) = \frac{\lambda_1}{2} \exp\left(\frac{\lambda_1(\lambda_1\sigma^2 + 2y)}{2}\right) \cdot \mathrm{erfc}\left(\frac{\lambda_1\sigma^2 + y}{\sqrt{2}\sigma}\right)$$

$\lambda_1 = \lambda / s$ lifetime / wind speed

Example of SO_2 near the smelters in Norilsk, Russia

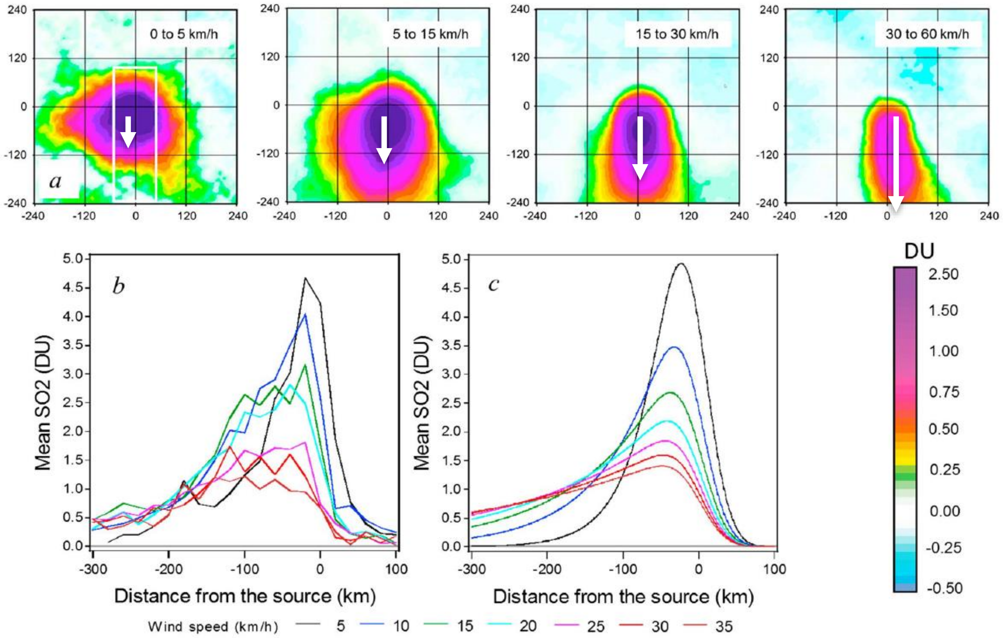

Dispersion and decay along y-axis (exponentially modified Gaussian)

Global SO_2 point source emissions

EUMETSAT

Empa
Materials Science and Technology

Fioletov et al., ACP 2020

- Quantification of SO_2 emissions from TROPOMI
- Large biases between SO_2 from TROPOMI, OMI and OMPS
- Biases removed for analysis
- TROPOMI has higher uncertainties per pixel but spatial averages are 2-3 times more accurate than for OMI

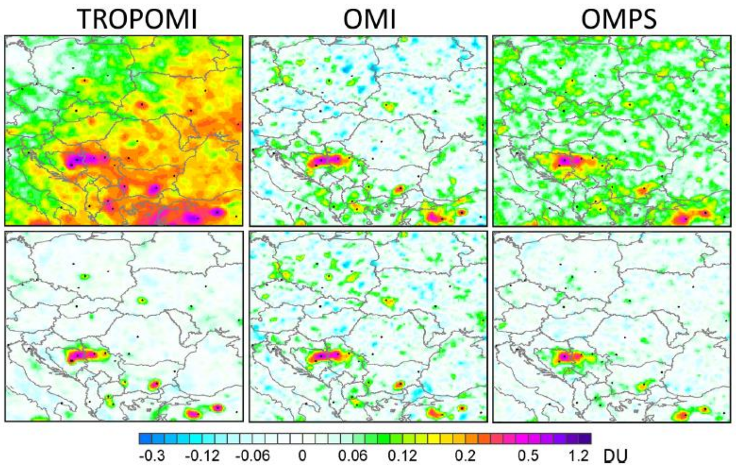

Original SO_2 columns

biases removed

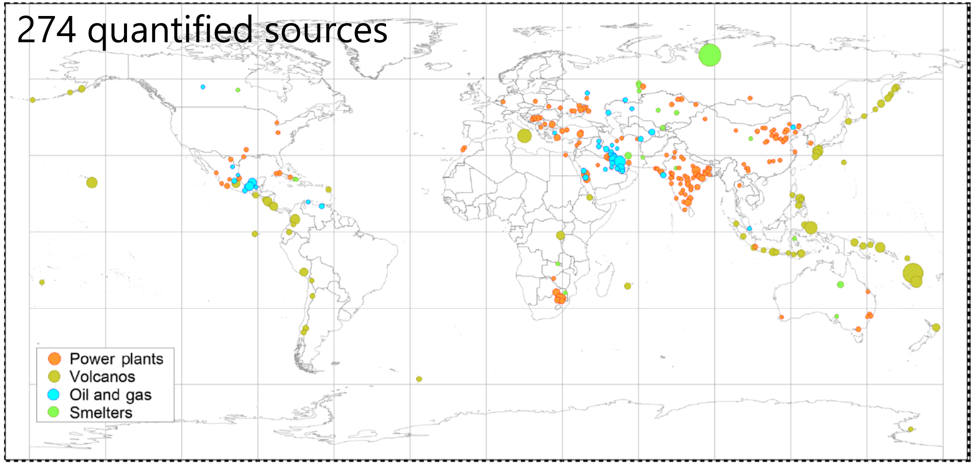

Global CH_4 emissions quantified from GOSAT

Maasakkers et al., ACP 2020

- Quantification of global CH_4 emissions and trends and OH from 2010-2015 using GOSAT observations
- Inverse modelling with GEOS-CHEM atmospheric transport model and more or less classical Bayesian inversion
- Ensemble of inversions to test sensitivity to different settings

Prior emissions from EDGAR 4.3.2, WetCHARTS, QFED

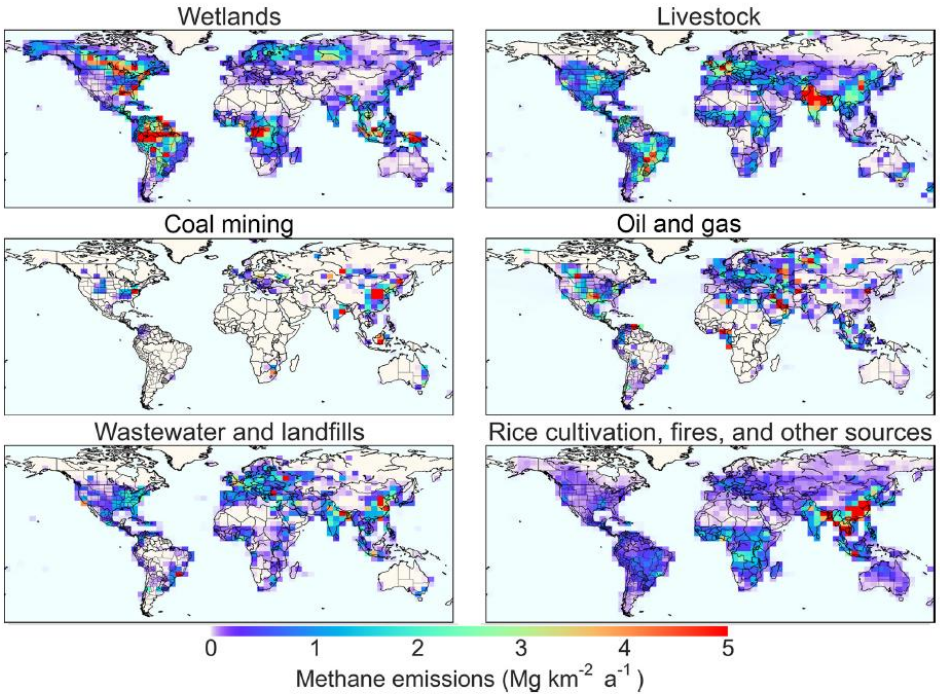

Global CH_4 emissions quantified from GOSAT

Maasakkers et al., ACP 2020

- Inversion optimizes emissions per grid cell
- Source-specific estimates obtained assuming the relative shares per grid cell are correct in prior

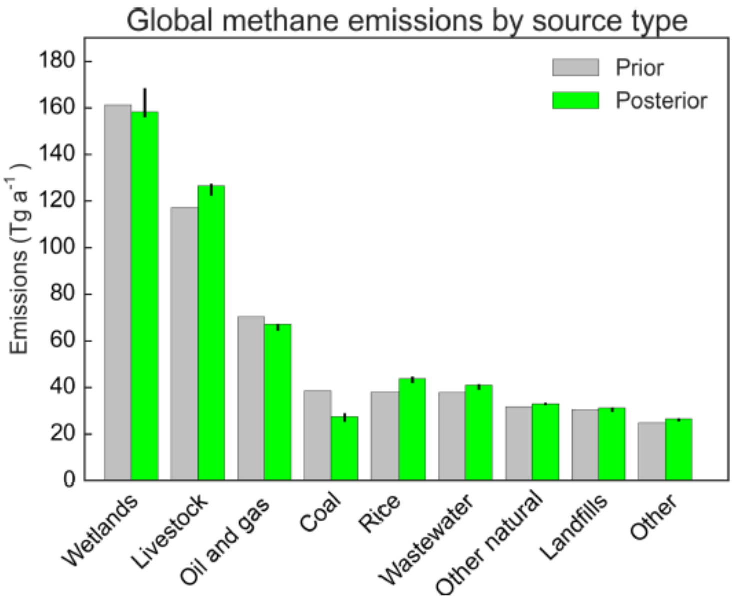

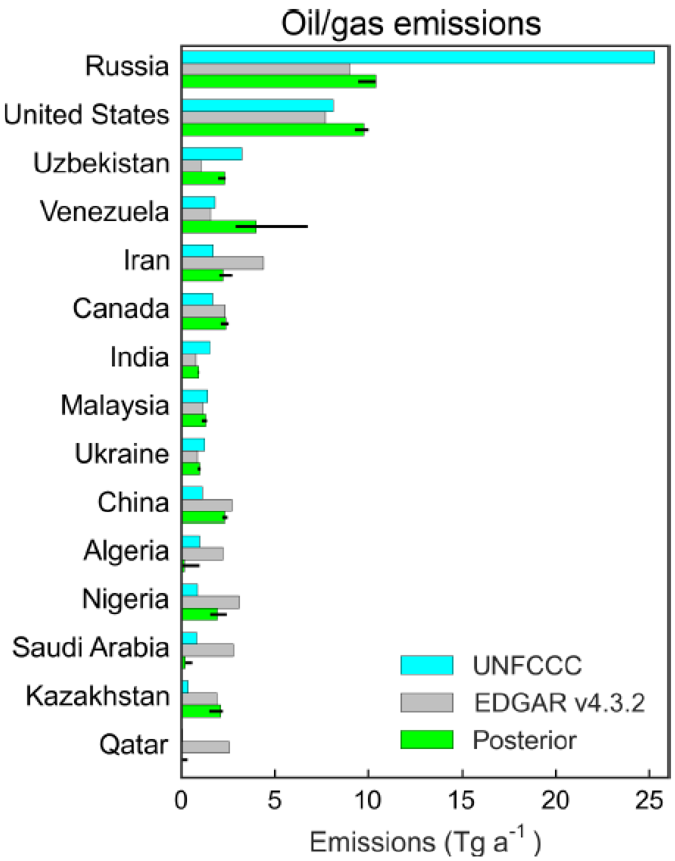

CO_2 emissions of cities and power plants

Kuhlmann et al. (2019, 2020 (in review)), Brunner et al. 2019

- OSSE study with synthetic CO_2 and NO_2 observations from future CO2M satellites
- High-resolution COSMO-GHG forward simulations
- Synthetic observations for constellations of up to 6 satellites
- Emissions estimated by mass balance and by analytical inversion

Synthetic CO2M XCO_2 and NO_2 observations (250-km swath)

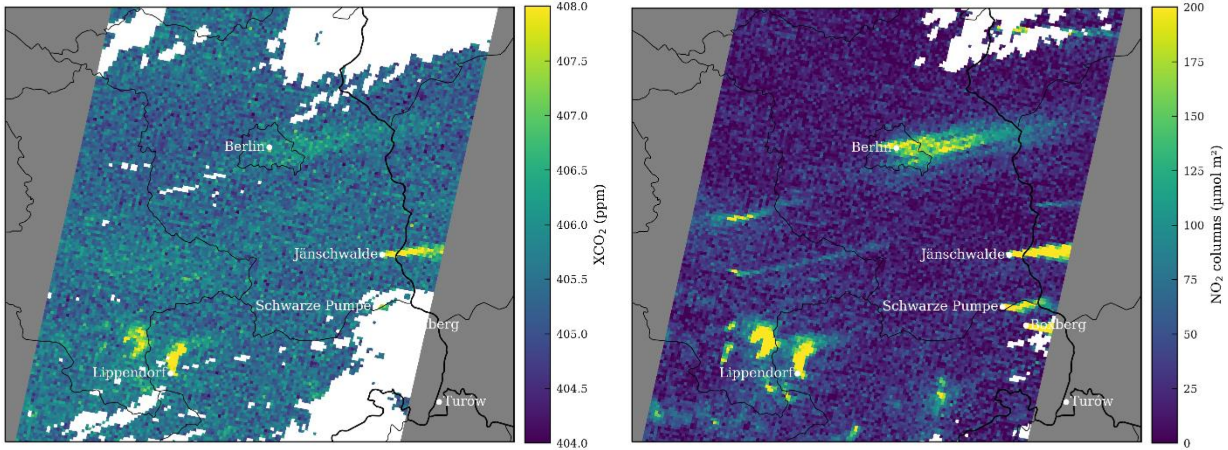

Plume detection for mass-balance approach
(Kuhlmann et al. 2019)

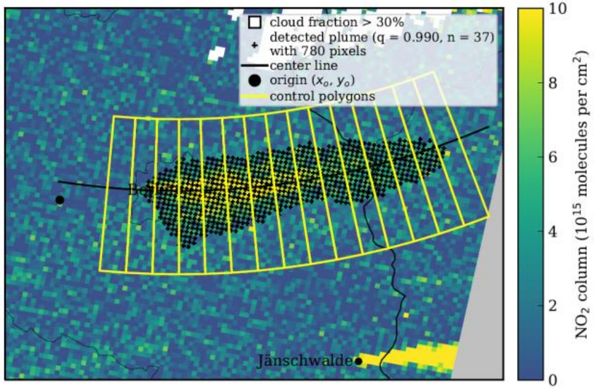

Berlin's emissions estimated from single overpasses

Analytical inversion (3 satellites)

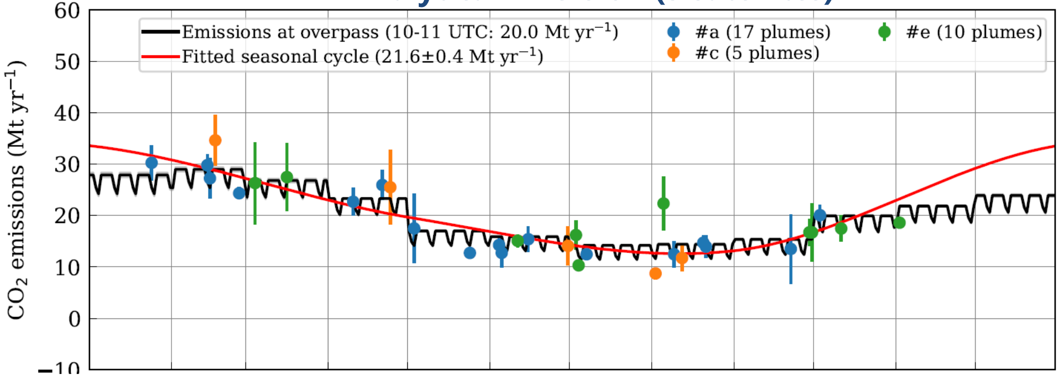

Mass-balance approach using NO_2 observations for plume detection

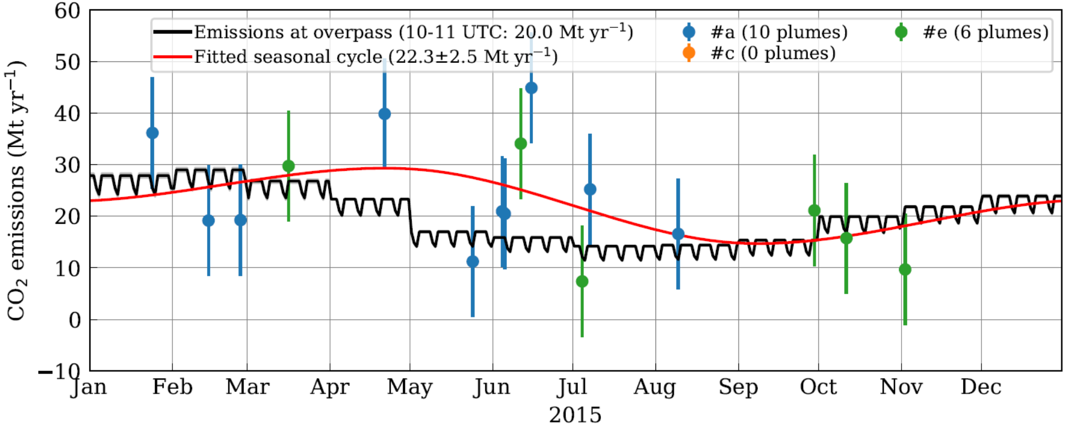

Mean bias and standard deviation wrt. true emissions at overpass time

	MB*	SD*
Analytical inversion	<1%	15-20%**
Mass-balance***	<25%	~50%

* 20 Mt CO_2 yr^{-1} at overpass (11:30 local time)
** for σ_{VEG50} of 0.5 to 1.0 ppm
*** also sensitive to emissions in vicinity of Berlin

Error budget of mass-balance approach

Error budget	MB	SD
Method error	<5%	~30%
Retrieval noise	<5-15%	10-30%
Background	-30*-15%**	30**-60%*
Wind	5-20%***	~30%

* CO_2 measurements (detected plume too small)
** NO_2 measurements (detects full city plume)
*** sensitive to plume length (vertical mixing)

Conclusions

- Detection of unknown sources ✓
- Quantification of emission hot spots ✓
- Estimates of relative share of individual emission sectors ✓ ✗
- Estimates of total emissions in political unit (country, county, city) ✓ ✗
- Changes during last few years (e.g. between reporting periods) ✓
- Long-term emission trends ✓ ✗

- Increasing resolution of satellites highly benefitial for source detection and quantification
- Results look often very impressive, but quality of top-down estimates often difficult to judge

Thank you for your attention